Antiviral Research 81 (2009) 267–276

Contents lists available at ScienceDirect

Antiviral Research

journal homepage: www.elsevier.com/locate/antiviral

Design, synthesis, molecular modeling, and anti-HIV-1 integrase activity of a series of photoactivatable diketo acid-containing inhibitors as affinity probes

Mario Sechi[a,*], Fabrizio Carta[a], Luciano Sannia[a], Roberto Dallocchio[b], Alessandro Dessì[b], Rasha I. Al-Safi[c], Nouri Neamati[c,**]

[a] Dipartimento Farmaco Chimico Tossicologico, Università di Sassari, Via Muroni 23/A, 07100 Sassari, Italy
[b] CNR-Istituto di Chimica Biomolecolare, Sassari, Trav. La Crucca 3, reg. Baldinca, 07040 Li Punti, Italy
[c] Department of Pharmacology and Pharmaceutical Sciences, University of Southern California, School of Pharmacy, 1985 Zonal Avenue, Los Angeles, CA 90089, USA

ARTICLE INFO

Article history:
Received 16 August 2008
Received in revised form 6 December 2008
Accepted 11 December 2008

Keywords:
HIV-1 integrase inhibitors
Diketo acids
Photoaffinity labeling
Photoprobes

ABSTRACT

The diketo acid (DKA) class of HIV-1 integrase (IN) inhibitors is thought to function by chelating divalent metal ions on the enzyme catalytic site. However, differences in mutations conferring resistance to various DKA inhibitors suggest that multiple binding orientations may exist. In order to facilitate identification of DKA binding sites, a series of photoactivable analogues of two potent DKAs was prepared as novel photoaffinity probes. In cross-linking assays designed to measure disruption of substrate DNA binding, the photoprobes behaved similarly to a reference DKA inhibitor. Molecular modeling studies suggest that such photoprobes interact within the IN active site in a manner similar to that of the parent DKAs. Analogues **Ia-c** are novel photoaffinity ligands useful in clarifying the HIV-1 binding interactions of DKA inhibitors.

1. Introduction

HIV-1 integrase (IN) is an attractive and validated target for developing novel antiretroviral agents (Neamati, 2001; Anthony, 2004; Pommier et al., 2005). Because of its vital role in the viral replication cycle, with no human counterpart of the enzyme known, the addition of an IN inhibitor to existing components of antiretroviral therapy (Barbaro et al., 2005) is expected to improve the outcome of therapy by potential synergism (De Clercq, 2002, 2005), without exacerbating toxicity (Cohen, 2002; Little et al., 2002).

In the past several years, a plethora of compounds with diverse structural features has been reported as IN inhibitors (Cotelle, 2006; Neamati, 2002). Several of them inhibit both the viral enzyme and viral replication in cell-based assays, as well as in animal models (Pommier et al., 2005). Among all the reported inhibitors, the β-diketo acid (DKA) class of compounds has shown the most promising results (Hazuda et al., 2000; Pais and Burke, 2002; Pommier et al., 2005). After about 15 years of study, the DKA-based derivative, Raltegravir (MK-0518, Plate 1), has been approved by the US Food and Drug Administration (Rowley, 2008; Wang et al., 2007). It is believed that the DKA pharmacophoric motif could be involved in a functional sequestration of one or both divalent metal ions that are critical cofactors at the enzyme catalytic site (Grobler et al., 2002; Pommier et al., 2005; Sechi et al., 2009). This would subsequently block the transition state of the IN-DNA complex (Espeseth et al., 2000). In this scenario it is of paramount importance to acquire information about the mode of action of DKAs that could then be useful in the design of new IN inhibitors.

Photoaffinity-labelling (PL) technology is emerging as a very useful tool for the identification and localization of proteins and their active sites in drug-discovery studies (Dormán and Prestwich, 2000; Fedan et al., 1984; Hatanaka and Sadakane, 2002; Kotzyba-Hibert et al., 1995). This method is particularly useful for the identification of ligand-binding sites of target proteins and for the investigation of ligand–receptor interactions. The use of affinity-labeled inhibitors to covalently modify the site of interaction and subsequent analysis of the protein has been very effective in providing useful information about inhibitor binding for a multitude of therapeutic target proteins. The PL technology enables the direct probing of a target protein through a covalent bond that is photochemically introduced between a ligand and its specific receptor (Fig. 1). Thus, PL could be applied in two levels of drug discovery and development processes. At macro-level, the method is useful for the screening of early leads from the evaluation of affinity by cross-linking, to know which ligand preferentially binds to which protein. If the binding site analysis of a target protein is important for defining a particular pharmacophore, the PL will give the structural information of receptor binding domain at the micro-level.

* Corresponding author. Tel.: +39 079 228 753; fax: +39 079 228 720.
** Corresponding author. Tel.: +1 323 442 2341; fax: +1 323 442 1390.
E-mail addresses: mario.sechi@uniss.it (M. Sechi), neamati@usc.edu (N. Neamati).

0166-3542/$ – see front matter © 2009 Elsevier B.V. All rights reserved.
doi:10.1016/j.antiviral.2008.12.010

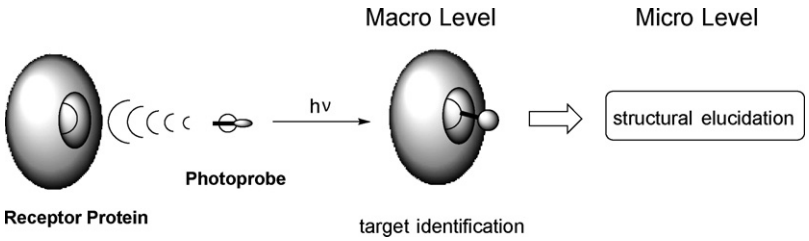

Fig. 1. The photoaffinity-labelling approach.

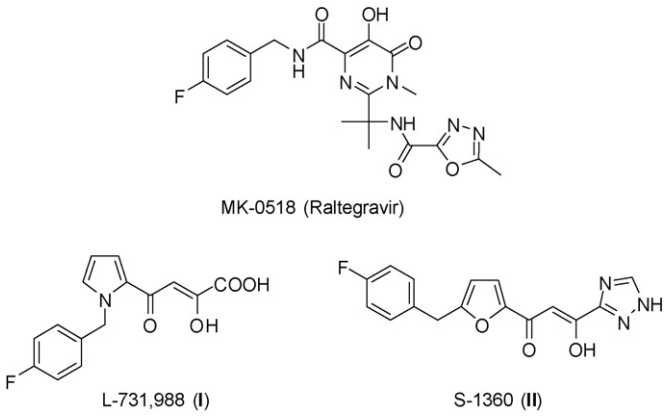

Plate 1. Structure of the first HIV-1 IN inhibitor in therapy (MK-0518), and representative diketo acid-based compounds, L-731,988 (**I**), S-1360 (**II**), used in this study.

Such an approach can be used to obtain structural information detailing the association between the enzyme IN and inhibitors under development. In fact, application of PL to IN has elucidated a small number of inhibitor-binding sites at atomic resolution (Al-Mawsawi et al., 2006).

To facilitate identification of DKA binding sites, a series of photoactivable compounds, related to two potent DKA-based inhibitors, L-731,988 (**I**) (Hazuda et al., 2000) and S-1360 (**II**, Plate 1) (Yoshinaga et al., 2002; Billich, 2003), was prepared as photoaffinity probes (Fig. 2). The latter were designed by replacing the para-fluoro-phenyl moieties of **I** and **II** with the three kinds of photophores, such as 4-azido-phenyl-, 4-azido-tetrafluorophenyl- and benzophenone, as photoreactive groups (Chehade and Spielmann, 2000; Dormán and Prestwich, 1994; Fleming, 1995). These photoprobes are expected to be useful tools for elucidation of the DKA binding mode and subsequent structure-based studies to design novel and selective IN inhibitors.

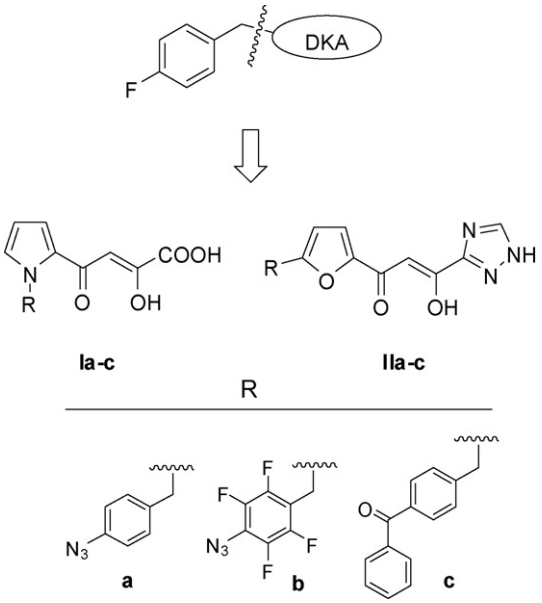

Fig. 2. Design of title compounds.

2. Materials and methods

2.1. Experimental chemistry

Anhydrous solvents and all reagents were purchased from Sigma–Aldrich, Merck or Carlo Erba. Anhydrous diethyl ether was obtained by distillation from Na/benzophenone under a nitrogen atmosphere. All reactions involving air- or moisture-sensitive compounds were performed under a nitrogen atmosphere using oven-dried glassware and syringes to transfer solutions. Melting points (mp) were determined using an electrothermal melting point or a Köfler apparatus and are uncorrected. Infrared (IR) spectra were recorded as thin films or nujol mulls on NaCl plates with a Perkin-Elmer 781 IR spectrophotometer and are expressed in ν (cm^{-1}). Nuclear magnetic resonance (^1H NMR, ^{13}C NMR, NOE difference and NOESY) spectra were determined in $CDCl_3$, DMSO-d_6 or $CDCl_3$/DMSO-d_6 (in 3/1 ratio) and were recorded at 200 MHz on a Varian XL-200. Chemical shifts (δ scale) are reported in parts per million (ppm) downfield from tetramethylsilane (TMS) used as an internal standard. Splitting patterns are designated as follows: s, singlet; d, doublet; t, triplet; q, quadruplet; m, multiplet; brs, broad singlet; dd, double doublet. The assignment of exchangeable protons (O*H* and N*H*) was confirmed by the addition of D_2O. Analytical thin-layer chromatography (TLC) was carried out on Merck silica gel F-254 plates. Flash chromatography purifications were performed on Merck Silica gel 60 (230–400 mesh ASTM) as the stationary phase. Elemental analyses were performed on a Perkin-Elmer 2400 spectrometer at Laboratorio di Microanalisi, Dipartimento di Chimica, Università di Sassari (Italy), and were within ±0.4% of the theoretical values.

2.1.1. General procedure for the preparation of photoprobes ***[Ia-c]***

A solution of the appropriate β-diketo ester **1a-c** (1 mmol) in MeOH (10 mL) was treated with 2N NaOH (4.0 eq) and was stirred at r.t. for 5 h. Then, the reaction mixture was diluted with water and acidified with 1N HCl. The yellow precipitate formed was filtered off, washed with water and recrystallized from H_2O/EtOH.

*2.1.1.1. 4-[1-(4-Azidobenzyl)-1H-pyrrol-2-yl]-2-hydroxy-4-oxobut-2-enoic acid **[Ia]***. Yield: 50%; mp 171–173 °C dec. IR (nujol): ν (cm^{-1}) 2113 (N_3 azide), 1719 (C=O acid), 1624 (C=O ketone). ^1H NMR (200 MHz, $CDCl_3$ + DMSO-d_6): δ 7.21–6.89 (m, 6H, Ar–H), 6.86 (s, 1H, CH=C), 6.35–6.22 (m, 1H, Ar–H, pyrrole), 5.61 (s, 2H, CH_2). MS: *m*/*z* 312 (M^+). Anal. Calc. for ($C_{15}H_{12}N_4O_4$): C, 57.69; H, 3.87; N, 17.94. Found: C, 57.55; H, 3.79; N, 18.03.

*2.1.1.2. 4-[1-(4-Azido-2,3,5,6-tetrafluorobenzyl)-1H-pyrrol-2-yl]-2-hydroxy-4-oxobut-2-enoic acid **[Ib]**.* Yield: 18%; mp 168–170 °C dec. IR (nujol): ν (cm^{-1}) 2100 (N_3 azide), 1707 (C=O acid), 1635 (C=O ketone). ^1H NMR (200 MHz, $CDCl_3$ + DMSO-d_6): δ 7.70–7.25 (m, 1H, Ar–H, pyrrole), 7.05–6.75 (m, 1H, Ar–H, pyrrole), 6.44–6.13 (m, 1H, Ar–H, pyrrole), 5.81 (s, 1H, CH=C), 3.72 (s, 2H, CH_2). MS: *m/z* 384 (M^+). Anal. Calc. for ($C_{15}H_8F_4N_4O_4$): C, 46.89; H, 2.10; N, 14.58. Found: C, 47.01; H, 2.03; N, 14.37.

*2.1.1.3. 4-[1-(4-Benzoylbenzyl)-1H-pyrrol-2-yl]-2-hydroxy-4-oxobut-2-enoic acid **[Ic]**.* Yield: 17%; mp 242–244 °C dec. IR (nujol): ν (cm^{-1}) 1721 (C=O acid), 1619 (C=O ketone). ^1H NMR (200 MHz, $CDCl_3$): δ 7.82–7.72 (m, 3H, Ar–H), 7.60–7.40 (m, 4H, Ar–H), 7.24–7.09 (m, 4H, Ar–H), 6.93 (s, 1H, CH=C), 6.36 (m, 1H, Ar–H), 5.71 (s, 2H, CH_2). MS: *m/z* 375 (M^+). Anal. Calc. for ($C_{22}H_{17}NO_5$): C, 70.39; H, 4.56; N, 3.73. Found: C, 70.57; H, 4.48; N, 3.67.

*2.1.2. General procedure for the preparation of β-diketo esters **[2a-c]***

To a suspension of 60% NaH in mineral oil (5.0 mmol) in dry Et_2O (10 mL) the corresponding ketone **1a-c** (1.7 mmol) was added and the reaction mixture was stirred under a nitrogen atmosphere at room temperature (r.t.) for 15 min. Then, dimethyloxalate (2.0 eq) was added and the reaction was stirred at r.t. for 3.5 h and at 50 °C for 12 h. Finally, the reaction was quenched with water and acidified with 2N HCl to afford a brown yellow precipitate.

*2.1.2.1. Methyl 4-[1-(4-azidobenzyl)-1H-pyrrol-2-yl]-2-hydroxy-4-oxobut-2-enoate **[2a]**.* Yield: 67%; mp 112–114 °C dec. IR (nujol): ν (cm^{-1}) 2113 (N_3 azide), 1727 (C=O ester), 1624 (C=O ketone). ^1H NMR (200 MHz, $CDCl_3$): δ 14.50 (brs, 1H, enol), 7.20–6.90 (m, 6H, Ar–H, benzyl and pyrrole), 6.84 (s, 1H, CH=C), 6.35–6.22 (m, 1H, Ar–H, pyrrole), 5.60 (s, 2H, CH_2). MS: *m/z* 326 (M^+). Anal. Calc. for ($C_{16}H_{14}N_4O_4$): C, 58.89; H, 4.32; N, 17.17. Found: C, 59.04; H, 4.23; N, 16.93.

*2.1.2.2. Methyl 4-[1-(4-azido-2,3,5,6-tetrafluorobenzyl)-1H-pyrrol-2-yl]-2-hydroxy-4-oxobut-2-enoate **[2b]**.* Yield: 20%; mp 108–110 °C dec. IR (nujol): ν (cm^{-1}) 2106 (N_3 azide), 1746 (C=O ester), 1638 (C=O ketone). ^1H NMR (200 MHz, $CDCl_3$): δ 14.44 (brs, 1H, enol), 7.16–7.10 (m, 1H, Ar–H, pyrrole), 7.00–6.94 (m, 1H, Ar–H, pyrrole), 6.84 (s, 1H, CH=C), 6.31–6.23 (m, 1H, Ar–H, pyrrole), 5.79 (s, 2H, CH_2), 3.92 (s, 3H, CH_3). MS: *m/z* 398 (M^+). Anal. Calc. for ($C_{16}H_{10}F_4N_4O_4$): C, 48.25; H, 2.53; N, 14.07. Found: C, 47.85; H, 2.69; N, 14.43.

*2.1.2.3. Methyl 4-[1-(4-benzoylbenzyl)-1H-pyrrol-2-yl]-2-hydroxy-4-oxobut-2-enoate **[2c]**.* Yield: 20%; mp 138–140 °C dec. IR (nujol): ν (cm^{-1}) 1731 (C=O ester), 1640 (C=O ketone). ^1H NMR (200 MHz, $CDCl_3$): δ 14.47 (brs, 1H, O*H*, exchange with D_2O), 7.83–7.65 (m, 3H, Ar–H), 7.62–7.41 (m, 4H, Ar–H), 7.22–7.05 (m, 4H, Ar–H), 6.86 (s, 1H, CH=C), 6.39–6.30 (m, 1H, Ar–H, pyrrole), 5.73 (s, 2H, CH_2), 3.91 (s, 3H, OCH_3). MS: *m/z* 389 (M^+). Anal. Calc. for ($C_{23}H_{19}NO_5$): C, 70.94; H, 4.92; N, 3.60. Found: C, 71.23; H, 4.83; N, 3.49.

*2.1.3. General procedure for the preparation of 1-[1-(4-alkyl)-1H-pyrrol-2-yl]ethanones **[1a-c]***

2-Acetylpyrrole **4** (2.83 mmol) was added to a suspension of KOH (4.0 eq) in dry DMSO (20 mL) and the reaction mixture was stirred at r.t. for 45 min. Then, the appropriate benzyl bromide **5a-c** (2.0 eq) was added, and the reaction was stirred for 2 h at r.t. The reaction was quenched with water and extracted with diethyl ether. The combined organic layers were dried over sodium sulfate, filtered and concentrated *in vacuo* to give a yellow oil (**1a**,**b**) or a yellow solid (**1c**) that was purified by silica gel column chromatography (eluting with petrol ether/ethyl acetate 9/1 for (**1a**,**b**) or with an increasing amount of petrol ether/ethyl acetate from 8.5/1.5 to 8/2 for (**1c**) to afford a pale yellow oil (**1a**,**b**) or a yellow solid (**1c**), respectively.

*2.1.3.1. 1-[1-(4-Azidobenzyl)-1H-pyrrol-2-yl]ethanone **[1a]**.* Yield: 80%; oil at r.t. IR (nujol): ν (cm^{-1}) 2108 (N_3 azide), 1660 (C=O ketone). ^1H NMR (200 MHz, $CDCl_3$): δ 7.11 (d, 2H, Ar–H), 7.05–6.86 (m, 4H, Ar–H, benzyl and pyrrole), 6.25–6.15 (m, 1H, Ar–H, pyrrole), 5.53 (s, 2H, CH_2), 2.41 (s, 3H, CH_3). MS: *m/z* 240 (M^+).

*2.1.3.2. 1-[1-(4-Azido-2,3,5,6-tetrafluorobenzyl)-1H-pyrrol-2-yl]ethanone **[1b]**.* Yield: 37%; oil at r.t. IR (nujol): ν (cm^{-1}) 2109 (N_3 azide), 1625 (C=O ketone). ^1H NMR (200 MHz, $CDCl_3$): δ 7.02–6.94 (m, 1H, Ar–H, pyrrole), 6.87–6.81 (m, 1H, Ar–H, pyrrole), 6.22–6.12 (m, 1H, Ar–H, pyrrole), 5.73 (s, 2H, CH_2), 2.44 (2, 3H, CH_3). MS: *m/z* 312 (M^+).

*2.1.3.3. 1-[1-(4-Benzoylbenzyl)-1H-pyrrol-2-yl]ethanone **[1c]**.* Yield: 45%; 86–88 °C dec. IR (nujol): ν (cm^{-1}) 1660 (C=O ketone). ^1H NMR (200 MHz, $CDCl_3$): δ 7.83–7.71 (m, 3H, Ar–H), 7.60–7.54 (m, 2H, Ar–H), 7.52–7.41 (m, 2H, Ar–H), 7.20–7.16 (m, 1H, Ar–H), 7.15–7.12 (m, 1H, Ar–H), 7.08–7.02 (m, 1H, Ar–H), 7.08–6.92 (m, 1H, Ar–H), 6.24 (dd, 1H, Ar–H), 5.66 (s, 2H, CH_2), 2.42 (s, 3H, CH_3). MS: *m/z* 303 (M^+).

*2.1.4. Synthesis of 1-(1H-pyrrol-2-yl)ethanone **[4]** (Sechi et al., 2006)*

A solution of 2-acetylfuran **3** (45.0 mmol) and 30% aqueous NH_3 (19.0 eq) in EtOH (30 mL) was heated into a sealed tube at 160 °C for 12 h. Then, the reaction mixture was cooled to r.t., filtered and the filtrate was concentrated *in vacuo* to give a brown solid. The latter was purified by silica gel column chromatography eluting with petroleum Et_2O/ethyl acetate 8/2 to afford a yellow solid that was crystallized from H_2O/EtOH. Yield: 75%; 88–89 °C (Lit. 88–89 °C) dec. IR (nujol): ν (cm^{-1}) 3260 (N*H*), 1640 (ketone). ^1H NMR (200 MHz, $CDCl_3$): δ 10.10 (brs, 1H, N*H*), 7.06–7.04 (m, 1H, Ar–H), 6.93–6.91 (m, 1H, Ar–H), 6.28–6.26 (m, 1H, Ar–H), 2.45 (s, 3H, $COCH_3$). MS: *m/z* 109 (M^+).

*2.1.5. Synthesis of 1-azido-4-(bromomethyl)benzene **[5a]***

A 1 M solution of PBr_3 in DCM (2.41 mmol) was added dropwise with a syringe to a solution of *p*-azido-benzylalcohol **7** (6.03 mmol) in dry DCM (18 mL) at 0–5 °C under a nitrogen atmosphere. The reaction mixture was stirred at r.t. for 3.5 h and then quenched with a mixture of 2-propanol (7.0 mL) in DCM (33.0 mL), followed by addition of 1 M $NaHCO_3$ (40 mL). The reaction mixture was extracted with DCM, and the combined organic layers were dried over sodium sulfate, filtered and the solvent was evaporated *in vacuo* to give a yellow oil that was purified by silica gel column chromatography eluting with petroleum ether to afford a yellow oil. Yield: 75%; oil at r.t. IR (nujol): ν (cm^{-1}) 2108 (N_3 azide), 1600 (C=C, Ar–C). ^1H NMR (200 MHz, $CDCl_3$): δ 7.37 (d, 2H, Ar–H), 6.99 (d, 2H, Ar–H), 4.48 (s, 2H, CH_2). MS: *m/z* 212 (M^+).

*2.1.6. Synthesis of (4-azidobenzyl)alcohol **[7]** (Griffin, 1996)*

A solution of sodium nitrite (30.5 mmol) was added portionwise to a solution of *p*-aminobenzylalcohol **6** (20.3 mmol) in 5N HCl (38 mL) at 0 °C and then NaN_3 (81.2 mmol) was added slowly. The reaction mixture was stirred at 0 °C for 1 h, then quenched with ice and adjusted to pH 8 with $NaHCO_3$. The mixture was extracted with ethyl acetate and the combined organic layers were dried over sodium sulfate, filtered and the solvent was removed *in vacuo* to give a yellow oil that was triturated with petroleum ether to afford a pale yellow solid. Yield: 92%; mp 32–34 °C dec. (Lit. 31–33 °C.) IR (nujol): ν (cm^{-1}) 2106 (N_3 azide), 1600 (C=C C–Ar). ^1H NMR

(200 MHz, $CDCl_3$): δ 7.35 (d, 2H, Ar–H), 7.02 (d, 2H, Ar–H), 4.67 (s, 2H, CH_2). MS: *m*/*z* 149 (M^+).

2.1.7. Synthesis of 1-azido-4-(bromomethyl)-2,3,5,6-tetrafluorobenzene ***[5b]*** *(Lei and Atkinson, 2000)*

A 1 M solution of PBr_3 in DCM (4.52 mL, 4.52 mmol) was added dropwise with a syringe to a solution of **11** (4.52 mmol) in dry DCM (16 mL) under a nitrogen atmosphere at 0–5 °C. The reaction mixture was stirred at r.t. for 4.5 h and quenched with a solution of 2-propanol (20 mL) in DCM (63 mL) followed by the addition of a 1 M aqueous solution of $NaHCO_3$ (82 mL). The mixture was extracted with DCM and the combined organic layers were dried over sodium sulfate, filtered and the solvent was removed *in vacuo* to give a yellow solid that was purified by silica gel column chromatography eluting with petroleum ether/ethyl acetate 9/1 to afford a pale yellow solid. Yield: 55%; mp 55–57 °C dec. (Lit. 53–55 °C.) IR (nujol): ν (cm^{-1}) 2110 (N_3 azide). ^{1}H NMR (200 MHz, $CDCl_3$): δ 4.50 (s, 2H, CH_2). MS: *m*/*z* 284 (M^+).

2.1.8. Synthesis of 4-azido-2,3,5,6-tetrafluorobenzylalcohol ***[11]*** *(Keana and Xiong Cai, 1990)*

A solution of $(CH_3)_2NH{\cdot}BH_3$ (1.2 eq) in acetic acid (25 mL) was added to a solution of **9** (13.7 mmol) in acetic acid (20 mL) and the reaction mixture was stirred at 60 °C for 1 h. Then, the reaction was quenched with water and extracted with chloroform and the combined organic layers were washed with a 5% aqueous solution of Na_2CO_3, dried over sodium sulfate, filtered and the solvent was removed *in vacuo* to give a white solid. Yield: 88%; mp 80–82 °C dec. (Lit. 67–68 °C.) IR (nujol): ν (cm^{-1}) 2108 (N_3 azide). ^{1}H NMR (200 MHz, $CDCl_3$): δ 4.79 (s, 2H, CH_2). MS: *m*/*z* 221 (M^+).

2.1.9. Synthesis of 4-azido-2,3,5,6-tetrafluorobenzaldehyde ***[9]*** *(Keana and Xiong Cai, 1990)*

NaN_3 (1.1 eq) was added to a solution of pentafluorobenzaldehyde **8** (25.5 mmol) in acetone (48 mL) and water (18 mL). The reaction mixture was stirred at reflux for 1 h. Then, the reaction was cooled down to r.t., water (60 mL) was added and it was extracted with diethyl ether. The combined organic layers were dried over sodium sulfate, filtered and the solvent was removed *in vacuo* to give a mixture of *para* and *ortho* isomers that were separated by silica gel column chromatography eluting with petroleum ether/ethyl acetate 9.5/0.5.

2.1.9.1. 4-Azido-2,3,5,6-tetrafluorobenzaldehyde ***[9]***. Yield: 66%; mp 45–47 °C dec. (Lit. 44–45 °C.) IR (nujol): ν (cm^{-1}) 2120 (N_3 azide), 1697 (C=O aldehyde). ^{1}H NMR (200 MHz, $CDCl_3$) δ 10.24 (s, 1H, CHO). ^{19}F NMR ($CDCl_3$): δ 150.8–151.1 (m, 2F), 144.7–145.0 (m, 2F). MS: *m*/*z* 219 (M^+).

2.1.9.2. 2-Azido-3,4,5,6-tetrafluorobenzaldehyde ***[10]***. Yield: 10%; mp 40–42 °C dec. IR (nujol): ν (cm^{-1}) 2121 (N_3 azide), 1712 (C=O aldehyde). ^{1}H NMR (200 MHz, $CDCl_3$) δ 10.24 (s, 1H, CHO). ^{19}F NMR ($CDCl_3$): δ 149.7 (d, 1F), 143.8–144.2 (m, 2F), 139.8 (d, 1F). MS: *m*/*z* 219 (M^+).

2.1.10. Synthesis of [4-(bromomethyl)phenyl](phenyl)methanone ***[5c]*** *(Zhao et al., 1997)*

Dibenzoylperoxide (0.122 mmol) was added to a mixture of **13** (3.06 mmol) and NBS (4.28 mmol) in carbon tetrachloride (16 mL). The reaction was refluxed for 76 h and then was cooled down to r.t., filtered and the solid obtained was washed with carbon tetrachloride. The filtrate was concentrated *in vacuo* to give a yellow solid that was purified by silica gel column chromatography eluting with petroleum ether/ethyl acetate 9.5/0.5 to afford a yellow solid. Yield: 69%; mp 109–111 °C dec. (Lit. 110–112 °C.) IR (nujol): ν cm^{-1} 1645 (C=O ketone). ^{1}H NMR (200 MHz, $CDCl_3$) δ 7.82–7.77 (m, 4H, Ar–H), 7.60–7.45 (m, 5H, Ar–H), 4.54 (s, 2H, CH_2). MS: *m*/*z* 275 (M^+).

2.1.11. Synthetic procedure for (4-methylphenyl)(phenyl)methanone ***[13]*** *(Gobbi et al., 2007)*

$AlCl_3$ (16.2 mmol) was added portion-wise to a solution of *p*-toluoylchloride **12** (6.47 mmol) in dry benzene (17.2 mL) cooled with an ice bath. The mixture was stirred at the same temperature for 1 h and at 60 °C for 2 h. Then, the reaction was cooled down to r.t., poured into 150 mL of 3N HCl and extracted with ethyl acetate. The combined organic layers were washed with water, dried over sodium sulfate, filtered and the solvent was removed *in vacuo* to give a yellow oil that solidifies at r. t. Yield: 98%; mp 48–50 °C dec. (Lit. oil.) IR (nujol): ν (cm^{-1}) 1663 (C=O ketone). ^{1}H NMR (200 MHz, $CDCl_3$) δ 7.81–7.76 (m, 4H, Ar–H), 7.58–7.43 (m, 5H, Ar–H), 2.44 (s, 3H, CH_3). MS: *m*/*z* 196 (M^+).

2.1.12. Synthesis of 1-[5-(4-fluorobenzyl)-2-furyl]ethanone ***[14]*** *(Short approach)*

To a solution of acetylfuran **3** (9.1 mmol) in dry DCM (4 mL) was added 1-(bromomethyl)-4-fluorobenzene **22** (13.7 mmol) followed by $FeCl_3$ 97% (2.73 mmol). After further addition of dry DCM (2 mL) the mixture was stirred at reflux for 48 h. Then, the reaction was cooled down to r.t. and quenched with water, extracted with DCM and the combined organic layers were washed with water, dried over sodium sulfate and filtered. The solvent was removed *in vacuo* to give a brown oil that was purified by silica gel column chromatography eluting with petroleum ether/ethyl acetate 8.5/1.5 to afford a pale yellow oil. Yield: 7%. Oil at r.t. IR (nujol): ν (cm^{-1}) 1672 (C=O ketone). ^{1}H NMR (200 MHz, $CDCl_3$) δ 7.24–7.18 (m, 2H, Ar–H), 7.09 (d, 1H, Ar–H furan), 7.04–6.98 (t, 2H, Ar–H), 6.09 (d, 1H, Ar–H furan), 4.01(s, 2H, CH_2), 2.43 (s, 3H, CH_3). MS: *m*/*z* 218 (M^+).

2.1.13. Synthesis of 1-[5-(4-fluorobenzyl)-2-furyl]ethanone ***[14]*** *(Longer approach)*

A 3 M solution of methylmagnesium bromide in diethyl ether (1.1 eq) was slowly added to a solution of **21** (5.27 mmol) in dry THF (58 mL) at 0 °C and under a nitrogen atmosphere. The reaction mixture was stirred at the same temperature for 1 h and then was quenched with a 10% aqueous solution of NH_4Cl and extracted with diethyl ether. The combined organic layers were dried over sodium sulfate, filtered and the solvent was removed *in vacuo* to give an orange oil that was purified by silica gel column chromatography eluting with petroleum ether/ethyl acetate 8/2 to afford a yellow oil. Yield: 54%. Oil at r.t. IR (nujol): ν (cm^{-1}) 1672 (C=O ketone). ^{1}H NMR (200 MHz, $CDCl_3$) δ 7.24–7.18 (m, 2H, Ar–H), 7.09 (d, 1H, Ar–H furan), 7.04–6.98 (t, 2H, Ar–H), 6.09 (d, 1H, Ar–H furan), 4.01(s, 2H, CH_2), 2.43 (s, 3H, CH_3). MS: *m*/*z* 218 (M^+).

2.1.14. Synthesis of S-pyridin-2-yl 5-(4-fluorobenzyl)furan-2-carbotioate ***[21]***

A mixture of triphenylphosphine (1.2 eq) and **20** (6.81 mmol) in dry acetonitrile (50 mL) was stirred at 10 °C for 1.5 h. Then the solvent was removed *in vacuo* to give a brown orange oil that was purified by silica gel column chromatography eluting with petroleum ether/ethyl acetate 8/2 to give a solid that was triturated from petroleum ether to afford an orange solid. Yield: 63%; mp 77–78 °C dec. IR (nujol): ν (cm^{-1}) 1649 (C=O ester). ^{1}H NMR (200 MHz, $CDCl_3$) δ 8.67–8.64 (m, 1H, Ar–H), 7.78–7.72 (m, 2H, Ar–H), 7.35–7.29 (m, 1H, Ar–H), 7.27–7.22 (m, 2H, Ar–H), 7.20 (d, 1H, Ar–H furan), 7.07–7.02 (m, 2H, Ar–H), 6.15 (d, 1H, Ar–H furan), 4.04 (s, 2H, CH_2). MS: *m*/*z* 313 (M^+).

2.1.15. Synthesis of 5-(4-fluorobenzyl)-2-furoic acid ***[20]***

A solution of NaI (5.0 eq) and chlorotrimethylsilane (5.0 eq) in dry acetonitrile (13 mL) was stirred at 0 °C under a nitrogen

atmosphere for 15 min. Then, a solution of **19** (9.31 mmol) in dry acetonitrile (33 mL) was slowly added and the reaction mixture was stirred at r.t. for 4 h. The reaction was quenched with water and extracted with ethyl acetate. The combined organic layers were washed with a solution of $Na_2S_2O_4{\cdot}5H_2O$ (2.1 eq) in water (22 mL) and brine, dried over sodium sulfate, filtered and the solvent was removed *in vacuo* to give a solid that was triturated from petroleum ether to afford an orange solid (yield 77%). mp 108–110 °C dec. IR (nujol): ν (cm^{-1}) 1672 (C=O acid). ^{1}H NMR (200 MHz, DMSO-d_6) δ 12.90 (brs, 1H, O*H*, exchange with D_2O), 7.33–7.26 (m, 2H, Ar–H), 7.15–7.11 (m, 3H, Ar–H, benzene and furan), 6.31 (d, 1H, Ar–H, furan), 4.05 (s, 2H, CH_2). MS: *m*/*z* 220 (M^+).

2.1.16. Synthesis of 5-[(4-fluorophenyl)(hydroxy)methyl]-2-furoic acid **[19]**

A solution of LDA [prepared from n-BuLi 2.5 M in *n*-hexane (21.4 mL, 53.6 mmol) and diisopropylamine (53.6 mmol) in dry THF (51 mL)] was stirred at −78 °C under a nitrogen atmosphere for 15 min. Then, a solution of furoic acid **18** (26.8 mmol) in dry THF (15 mL) was added and the reaction mixture was stirred at −78 °C for 30 min. *p*-Fluorobenzaldehyde **17** (26.8 mmol) was slowly added. The reaction mixture was stirred at the same temperature for 4 h, quenched with water, acidified with 3N HCl, and extracted with diethyl ether. The combined organic layers were evaporated *in vacuo* to give a yellow oil that was dissolved in ethyl acetate and extracted with a 5% aqueous solution of $NaHCO_3$. The combined basic aqueous layers were acidified with 3N HCl to afford a yellow oil that solidified and was triturated with petroleum ether/diethyl ether to give a pale yellow solid. Yield: 53%; mp 174–176 °C dec. IR (nujol): ν (cm^{-1}) 1694 (C=O acid). ^{1}H NMR (200 MHz, $CDCl_3$) δ 7.37–7.33 (m, 2H, Ar–H), 7.07 (d, 1H, Ar–H, furan), 6.99 (t, 2H, Ar–H), 6.06 (d, 1H, Ar–H, furan), 5.77 (s, 1H, CH). MS: *m*/*z* 236 (M^+).

2.1.17. Synthesis of ethyl 1-trityl-1H-1,2,4-triazol-5-carboxylate **[15]** (Norcross et al., 1997)

Triethylamine (2.21 mL) and chlorotriphenylmethane (8.43 mmol) were added to a solution of compound **26** (7.94 mmol) in dry DMF (27 mL) at r.t. The mixture was stirred for 15 min at r.t. and quenched with water. The precipitate formed was filtered and washed with water and diethyl ether to afford a white solid. Yield: 95%; mp 157–158 °C dec. IR (nujol): ν (cm^{-1}) 1739 (C=O ester). ^{1}H NMR (200 MHz, $CDCl_3$) δ 8.01 (s, 1H, Ar–H), 7.36–7.31 (m, 9H, Ar–H), 7.13–7.11 (m, 6H, Ar–H), 4.45 (q, 2H, CH_2), 1.41 (t, 3H, CH_3). MS: *m*/*z* 383 (M^+).

2.1.18. Synthesis of ethyl 1H-1,2,4-triazol-5-carboxylate **[26]** (Vanek et al., 1984)

A suspension of **25** (6.3 mmol) in diglyme (4 mL) was stirred at reflux for 1.5 h. Then, the reaction was cooled to r.t. and the precipitate formed was filtered and washed with *n*-hexane to give a white solid. Yield: 81%; mp 168–169 °C dec. (Lit. 176–178 °C.) IR (nujol): ν (cm^{-1}) 1713 (C=O ester). ^{1}H NMR (200 MHz, $CDCl_3$) δ 8.53 (s, 1H, Ar–H), 4.53 (q, 2H, CH_2), 1.47 (t, 3H, CH_3). MS: *m*/*z* 141 (M^+).

2.1.19. Synthesis of amino(formylhydrazo) ethyl acetate **[25]** (Vanek et al., 1984)

A mixture of ethyl thioxammate **24** (5.6 mmol) and formylhydrazine **23** (5.9 mmol) was heated at 65 °C for 1 h. The reaction then was cooled to r.t. and the solid formed was filtered and washed with ethanol to afford a pale yellow solid. Yield: 60%; mp 148–149 °C dec. (Lit. 159–160 °C.) IR (nujol): ν (cm^{-1}) 3311 (NH_2 primary amine), 3199 (NH amide), 1735 (C=O ester), 1645 (C=O amide). ^{1}H NMR (200 MHz, $CDCl_3$ + DMSO-d_6) δ 10.60–10.31 (m, 1H, N*H*, exchange with D_2O), 8.60 (d, 1H, C*H*O), 6.21 (s, 2H, NH_2, exchange with D_2O), 4.31 (q, 2H, CH_2), 1.35 (t, 3H, CH_3). MS: *m*/*z* 159 (M^+).

2.1.20. Synthesis of 1-[5-(4-fluorobenzyl)-2-furyl]-3-hydroxy-3-(1H-1,2,4-triazol-5-yl)prop-2-en-1-one **[II]** (**S-1360**)

HCl 3N (7.8 mL) was added to a solution of compound **16** (2.34 mmol) in 1,4-dioxane (30 mL) and the mixture was stirred at 80 °C for 30 min. Then the reaction was cooled to r.t. and the solvent was evaporated *in vacuo* to give a residue that was dissolved in diethyl ether and was extracted with 1N NaOH. The combined aqueous layers were acidified with 3N HCl and the precipitate formed was filtered and washed with water and ethyl acetate. The solid residue was crystallized from ethyl acetate to afford a yellow solid. Yield: 38%; mp 178–179 °C dec. IR (nujol): ν (cm^{-1}) 3580 (N*H* triazole). ^{1}H NMR (200 MHz DMSO-d_6) δ 8.77 (brs, 1H, N*H*, exchange with D_2O), 7.51 (d, 1H, Ar–H), 7.37–7.31 (m, 2H, Ar–H), 7.17 (t, 2H, Ar–H), 6.93 (s, 2H, CH), 6.47 (d, 1H, Ar–H), 4.15 (s, 2H, CH_2). MS: *m*/*z* 313 (M^+). Anal. Calc. for ($C_{16}H_{12}FN_3O_3$): C, 61.34; H, 3.86; N, 13.41. Found: C,60.89; H, 3.98; N, 13.65.

2.1.21. Synthesis of 1-[5-(4-fluorobenzyl)-2-furyl]-3-hydroxy-3-(1-trityl-1,2,4-triazol-5-yl)prop-2-en-1-one **[16]**

A 1 M solution of LHMDS in THF (3.87 mmol) was added at −70 °C to a solution of **14** (2.98 mmol) in THF (9 mL) under nitrogen atmosphere. The reaction mixture was slowly warmed to −10 °C and cooled to −70 °C. **15** (3.87 mmol) in THF (15 mL) was added and the reaction mixture was slowly warmed to r.t. and stirred at the same temperature for 1.5 h. The reaction was quenched with a 10% aqueous solution of NH_4Cl and was acidified with 3N HCl. The solution was extracted with ethyl acetate and the combined organic layers were washed with brine and dried over sodium sulfate, filtered and the solvent removed *in vacuo* to give an orange solid that was triturated from diethyl ether to afford a pale orange solid. Yield: 87%; mp 207–209 °C dec. IR (nujol): ν (cm^{-1}) 1624 (C=O ketone). ^{1}H NMR (200 MHz $CDCl_3$) δ 7.53–7.33 (m, 12H, Ar–H), 7.20–7.06 (m, 9H, Ar–H), 6.91 (s, 1H, CH), 6.47 (d, 1H, Ar–H), 4.14 (s, 2H, CH_2). MS: *m*/*z* 555 (M^+).

2.2. Biology

2.2.1. Materials, chemicals, and enzymes

All compounds were dissolved in DMSO and the stock solutions were stored at −20 °C. The γ [^{32}P]-ATP was purchased from either Amersham Biosciences or ICN. The expression systems for the wild-type IN was a generous gift of Dr Robert Craigie, Laboratory of Molecular Biology, NIDDK, NIH, Bethesda, MD.

2.2.2. Preparation of oligonucleotide substrates

The oligonucleotides 21-top, 5′-GTGTGGAAAATCTCTAGCAGT-3′ and 21-bot, 5′-ACTGCTAGAGATTTTCCACAC-3′ were purchased from Norris Cancer Center Microsequencing Core Facility (University of Southern California) and purified by UV shadowing on polyacrylamide gel. To analyze the extent of strand transfer using 5′-end labeled substrates, 21-top was 5′-end labeled using T_4 polynucleotide kinase (Epicentre, Madison, WI) and γ [^{32}P]-ATP (Amersham Biosciences or ICN). The kinase was heat-inactivated and 21-bot was added in 1.5 M excess. The mixture was heated at 95 °C, allowed to cool slowly to room temperature, and run through a spin 25 mini-column (USA Scientific) to separate annealed double-stranded oligonucleotide from unincorporated material.

2.2.3. Integrase assays

To determine the extent of strand transfer, wild-type IN was preincubated at a final concentration of 200 nM with the inhibitor

in reaction buffer (50 mM NaCl, 1 mM HEPES, pH 7.5, 50 μM EDTA, 50 μM dithiothreitol, 10% glycerol (w/v), 7.5 mM $MnCl_2$, 0.1 mg/mL bovine serum albumin, 10 mM 2-mercaptoethanol, 10% DMSO and 25 mM MOPS, pH 7.2) at 30 °C for 30 min. Then, 20 nM of the 5′-end ^{32}P-labeled linear oligonucleotide substrate was added, and incubation was continued for an additional 1 h. Reactions were quenched by the addition of an equal volume (16 μL) of loading dye (98% deionized formamide, 10 mM EDTA, 0.025% xylene cyanol and 0.025% bromophenol blue). An aliquot (5 μL) was electrophoresed on a denaturing 20% polyacrylamide gel (0.09 M tris-borate pH 8.3, 2 mM EDTA, 20% acrylamide, 8 M urea).

Gels were dried, exposed in a PhosphorImager cassette, and analyzed using a Typhoon 8610 Variable Mode Imager (Amersham Biosciences) and quantitated using ImageQuant 5.2. Percent inhibition (% I) was calculated using the following equation:

$$\%I = 100 \times \left[1 - \frac{D - C}{N - C}\right]$$

where *C*, *N*, and *D* are the fractions of 21-mer substrate converted to strand transfer products for DNA alone, DNA plus IN, and IN plus drug, respectively. The IC_{50} values were determined by plotting the logarithm of drug concentration *versus* percent inhibition to obtain the concentration that produced 50% inhibition.

2.3. Molecular modeling

Model compounds L-731,988 (**I**) and **Ia-c**, and S-1360 (**II**) and **IIa-c** were constructed with standard bond lengths and angles from the fragment database with MacroModel 6.0 using a Silicon Graphics O2 workstation running on IRIX 6.3. Sybyl 6.2 as graphic platform. The atomic charges were assigned using the Gasteiger–Marsili method (Gasteiger and Marsili, 1980). Minimization of structures was performed with the MacroModel/BachMin 6.0 program using the AMBER force field. An extensive conformational search was carried out using the Monte Carlo/energy minimization (Chang et al., 1989) for all the compounds considered in the study (*Ei-E*min <5 kcal/mol, energy difference between the generated conformation and the current minimum). Representative minimum energy conformations of each compounds were optimized using the *ab initio* quantum chemistry program Gaussian 98 with method B3LYP/6–311G basis set. Moreover, compounds **I** and **II** were submitted to quantum mechanics calculation by using B3LYP/6–311G method. Gaussian and docking calculations were performed on HP Exemplar Parallel Server V2200 running HP UX 11.0.

Subunit A of the IN core domain in complex with 1-(5-chloroindol-3-yl)-3-hydroxy-3-(2H-tetrazol-5-yl-propenone) (5CITEP; PDB 1QS4) (Goldgur et al., 1999) was used for all docking studies. The missing residues at positions 141–144 in this subunit were incorporated from monomer B of the IN structure PDB 1BIS after superimposition of the backbone residues 135–140 and 145–150, as previously reported (Sechi et al., 2004a; Sotriffer et al., 2000a,b). Docking was performed with AutoDock version 3.05 (Morris et al., 1996) using the new empirical free energy function and the Lamarckian protocol (Morris et al., 1998). Mass-centered grid maps were generated with 80 grid points for every direction,

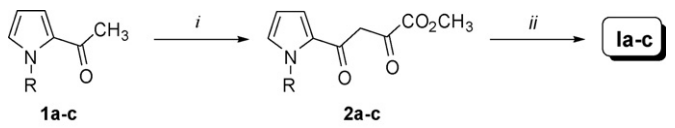

Scheme 1. Preparation of compound **I** (L-731,988) and photoprobes **Ia-c**.

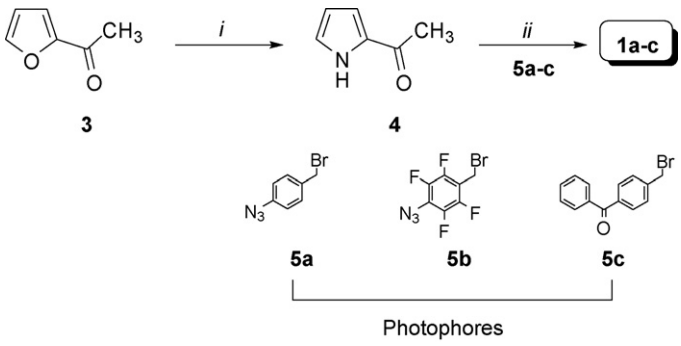

Scheme 2. Preparation of the ester intermediates **1** and **1a-c**.

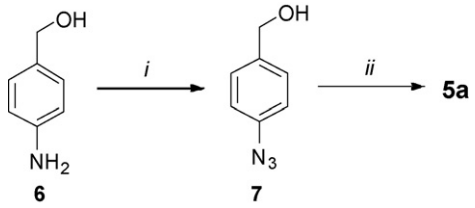

Scheme 3. Preparation of photophore **5a**.

and with 0.375 Angstroms spacing by the AutoGrid program for the whole protein target. Random starting position on the entire protein surface, random orientations, and torsions were used for the ligands. The distance-dependent dieletric permittivity of Mehler and Solmajer was used for the calculation of the electrostatic grid-maps. 100 independent docking runs were carried out for each ligand. The cluster analysis was computed with a cluster tolerance at less than 1.5 Å in positional root-mean-square deviation.

3. Results and discussion

3.1. Chemistry

We used a common synthetic strategy to prepare the target compounds **Ia-c** and **IIa-c**. Synthetic approaches for the preparation of reference compounds **I** and **II** and the photolabeled derivatives **Ia-c** are depicted in Schemes 1–8.

DKAs **Ia-c** were obtained following the same procedure already used for the preparation of the reference compound **I**. In particular, **Ia-c** were obtained by alkaline hydrolysis of their respective β-diketo esters **2a-c**. The latter were synthesized by Claisen condensation of the appropriate acetyl-derivatives **1a-c** with

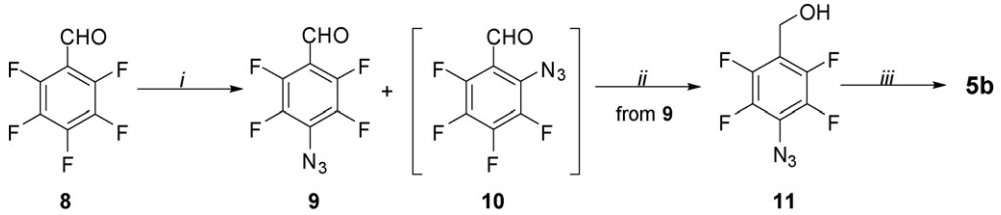

Scheme 4. Preparation of photophore **5b**.

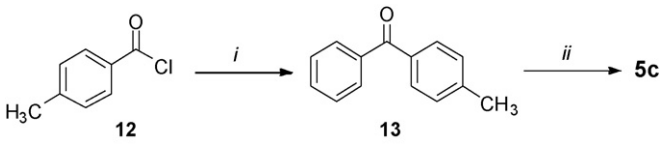

Scheme 5. Preparation of photophore **5c**.

dimethyloxalate in the presence of sodium hydride in anhydrous DMF (Scheme 1). The intermediates **1a-c** were easily obtained by adapting a method previously reported by our group (Sechi et al., 2004b, 2006). Pyrrolization of 2-acetylfuran **3** with 30% acqueous NH_3 in sealed tube at 160 °C afforded the intermediate **4** in good yield. Alkylation of the 2-acetylpyrrole **4** with the appropriate benzylbromide in powdered KOH/DMSO gave the corresponding alkylpyrrole **1a-c** (Scheme 2). The photophore 4-azide-benzylbromide **5a** was obtained by a Sandmeyer reaction of the aminobenzylalcohol **6** to give the azidobenzylalcohol **7** (Griffin, 1996), which was converted to the desired benzylbromide **5a** using PBr_3 (Scheme 3).

The tetrafluoroarylazide **5b** was prepared by substitution of the fluorine in 4-position of the pentafluorobenzaldehyde **8** with NaN_3 to give **9** (Keana and Xiong Cai, 1990) (with a small amount of the orto-isomer **10**), followed by a reduction of the aldehyde group with dimethylamonoborane to afford the alcohol **11**. The latter was then brominated in the presence of PBr_3 in CH_2Cl_2 to give the desired benzylbromide **5b** (Lei and Atkinson, 2000) (Scheme 4). Then, the photophore benzophenone **5c** was synthesized by a Friedel–Craft acylation of the *p*-tolylchloride **12** with benzene to give the benzophenone **13** (Smith, 1921), which was brominated with NBS and catalytic dibenzoyl peroxide to afford the benzyl bromide **5c** (Tanaka et al., 1998) (Scheme 5).

Another goal was to prepare the reference compound, S-1360 (**II**), in order to find a versatile synthetic route that could be used for the preparation of the photoprobes **IIa-c**. The preparation of **II** was formally the same as used for **Ia-c**, which followed a Claysen-type reaction between the synthones **14** and **15**. Both synthones were then coupled by treating with 1 M LHMDS at −70 °C to give the protected compound **16** in 87% yield (Scheme 6). Hydrolysis of the trityl group by 3N HCl gave the desired **II**.

The synthon **14** was prepared by reacting the acid **20** with dipyridyldisulfide in the presence of Ph_3P to give the thioate **21**, which, after treating with 3 M CH_3MgBr (Araki et al., 1974), afforded **14** in good yield (Scheme 7A). Interestingly, the acid intermediate **20** was also obtained by a tandem-reaction between the *p*-fluorobenzaldehyde **17** and the 2-furoic acid **18** using 1.8 M LDA in THF (Knight, 1979) to give the alcohol **19**, followed by reduction in the presence of TMSCl and NaI (Stoner et al., 1995) (Scheme 7A). We also obtained the desired synthon **14** by a direct alkylation between the benzylbromide **22** and the 2-acetylfuran **3**, albeit in low yield (Scheme 7B).

The synthon **15** was synthesized by heating both the formylhydrazine **23** and the thioamide **24** to give the acylamidrazone **25** (Vanek et al., 1984). The latter was refluxed in diglyme to give

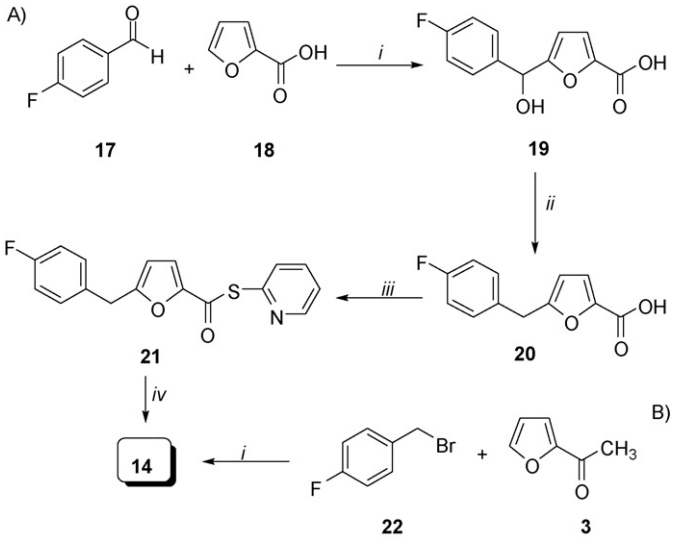

Scheme 7. Preparation of synthon **7**.

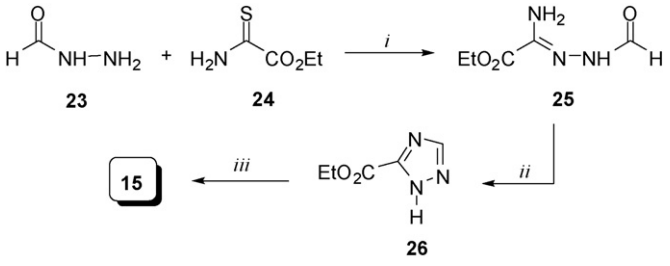

Scheme 8. Preparation of synthon **8**.

the acetyltriazole **26**, which was protected with chlorotriphenylmethane (Norcross et al., 1997) to give **15** in high yield (Scheme 8).

3.2. Biology

The photoprobes **Ia-c** were tested for their ability to inhibit IN catalytic activities in in vitro assays employing purified enzyme. All tested compounds showed anti-IN activity in the low micromolar concentration range. All the compounds of the L-731,988 series inhibited strand transfer reactions with IC_{50} values of <3.7 μM, while the inhibition values against the 3′-processing catalytic step were in a range from 12 to 28 μM. Ideally, the photoprobe should be bioactive in the same range as its parent compound, but compounds with as much as 1000 times lower activity can still be useful. In our case it was observed that, in cross-linking assays designed to measure disruption of substrate DNA binding, the photoprobes behaved similarly to a reference DKA inhibitor (IC_{50s} = <3.7 μM and 0.54 ± 0.08 against strand transfer, for **Ia-c** and **I**, respectively). Therefore, photoprobes **Ia-c** were selected for further photoaffinity

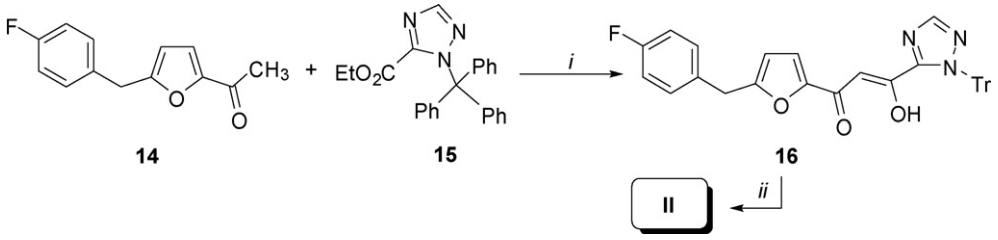

Scheme 6. Preparation of compound **II** (S-1360).

labelling studies employing full-length and catalytic core (residues 50–212) units of IN in the presence and absence of substrate DNA, using UV-cross-linking followed by enzyme digestion, separation, and mass spectrometry as recently described (Al-Mawsawi et al., 2006). Studies are in progress for finalizing a general scheme for DKA binding sites.

3.3. Molecular modeling

We performed detailed docking studies to predict interaction of **I** and **II** and their corresponding photoprobes into the active site of IN. In the absence of key, relevant crystal structures, molecular modeling has been used extensively to assist the understanding of the binding of inhibitors to the IN active site and to aid in the design of novel inhibitors. (Barreca et al., 2003; Chen et al., 2002; Sotriffer et al., 2000a,b; Zeinalipour-Loizidou et al., 2007.) Previously, an X-ray structure of one DKA analogue (5CITEP) has been crystallized with the enzyme (Goldgur et al., 1999). To investigate the putative binding modes of the title compounds **Ia-c**, compared with those of the reference compound **I**, we used the IN-5CITEP complex (PDB 1QS4) as described (Sechi et al., 2004a; Sotriffer et al., 2000a,b). Considering that the carboxylic group of DKAs has a pK_a of ~4 under physiological conditions (Sechi et al., 2006) we modeled L-731,988 and related photoprobes as carboxylates for docking studies. Moreover, since the triazole has a pK_a of ~9 (Woodruf and Polya, 1975), we considered the S-1360 and its related photoprobes in the neutral form.

Graphical representations of top-ranking binding modes obtained for these ligands showing the important residues involved in binding are depicted in Figs. 3 and 4. The results of clustered docking runs with the most favorable free binding energy are given in Table 1.

According to docking results, the amino acid residues involved in the binding of title compounds located near the catalytic site were as follows: Asp64, Cys65, His67, Asp116, Ser119, Asn120, Gln148, Asn155, Lys156 and Lys159. Several of these were considered to be very important for the activity of IN, and some have been previously shown to play a role in substrate binding (Neamati et al., 2000; Semenova et al., 2008; Sotriffer et al., 2000b). In general, a similar mode of binding with the same orientation on the active site was observed for the ligands of each series. In fact, **I** and **Ia-c** as well as **II** and **IIa-c** show an overlapping orientation in the enzyme site. In particular, we found that **I** and **Ia-c** bind within the following amino acid pattern: Cys65, His67, Asp116, Gln148, and Asn155. Moreover, they chelate Mg^{2+}, involving both the 2-enol and carboxylate functionalities (Fig. 3). As far as the disposition of **II** and photoprobes **IIa-c** are concerned, they form a planar conformation and achieve favorable interactions with various amino acid residues, such as Asp64, Ser119, Asn120, Asn155, Lys156 and Lys159. In this bound orientation, two oxygen atoms, the oxygen atom in the furan ring and keto group, form coordinate bonds with Mg^{2+} ion, as already observed (Dayam and Neamati, 2004) (Fig. 4).

Table 1
Docking results of 100 independent runs for compounds **I**, **Ia-c**, **II**, **IIa-c**.

Ligand	N_{tot}[a]	f_{occ}[b]	ΔG_{bind}[c]	H-bonds
I	5	19/11	−8.87	His 67, Gln 148, Asn 155
Ia	6	26/13	−9.64	Asp 116, Gln 148, Asn 155
Ib	6	34/15	−9.82	Cys 65, His 67, Gln 148
Ic	7	51/24	−9.20	Cys 65, Gln 148
II	5	21/9	−7.75	Ser 119, Asn 120, Lys 159
IIa	6	34/14	−8.11	Ser 119, Asn 120, Lys 156, Lys 159
IIb	6	35/14	−8.68	Ser 119, Asn 120, Asn 155, Lys 156, Lys 159
IIc	7	31/15	−7.23	Asp 64, Asn 155, Lys 156

[a] Total number of clusters.
[b] Number of distinct conformational clusters found out of 100 runs/number of multi-member conformational clusters.
[c] Estimated free binding energy (kcal/mol).

The estimated free binding energy values (ΔG_{bind}) of the docked positions, expressed in kcal/mol, indicated favorable interactions and tight binding with key amino acid residues at the active site of IN. Photoprobes **Ia-c** showed similar free binding energy, when compared with the reference compound **I** (ΔG_{bind} = −9.64, −9.82, −9.20 and −8.87 kcal/mol for **Ia**, **Ib**, **Ic** and **I**, respectively). High free binding energy values have also been obtained for the reference compound **II** and its related photoprobes (Table 2).

Then, we performed calculation of electronic density with the aim of understanding how structural changes can affect substrate

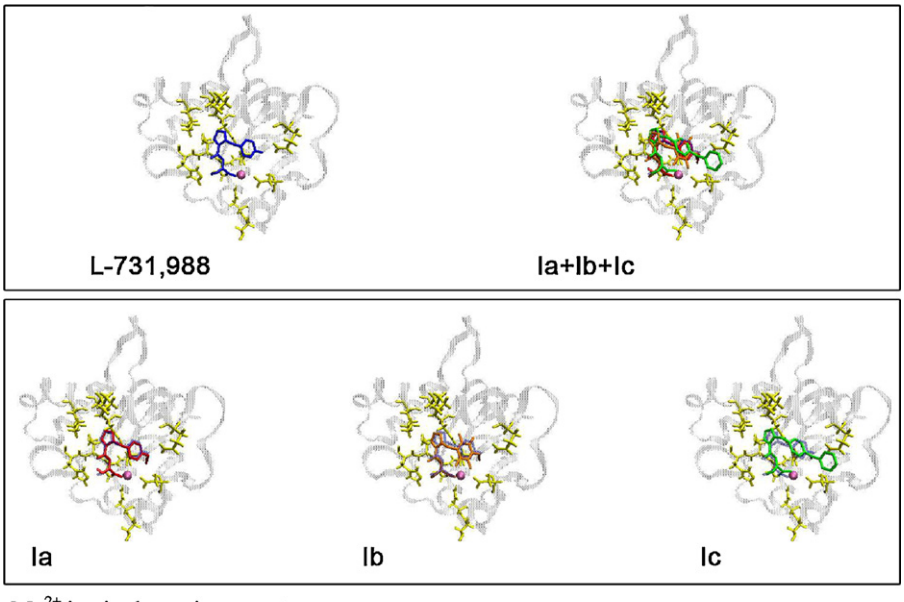

Fig. 3. Graphical representation of hypothetical disposition of **I** (blue) and **Ia-c** showing the interacting amino acid residues on the HIV-1 IN active site core domain. **Ia** + **Ib** + **Ic** displayed the overlap of both conformers. **Ia** (red) as well as **Ib** (orange) and **Ic** (green) represent the top and conformation derived from the docking results for each monomer (overlapped with **I**), respectively. (For interpretation of the references to colour in this figure legend, the reader is referred to the web version of the article.)

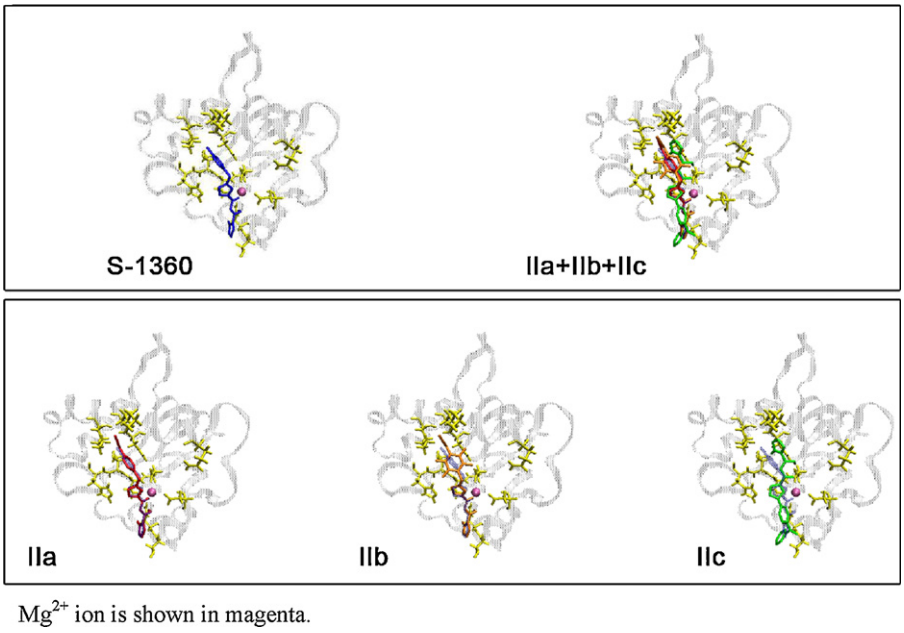

Fig. 4. Graphical representation of hypothetical disposition of **II** (blue) and **IIa-c** showing the interacting amino acid residues on the HIV-1 IN active site core domain. **IIa** + **IIb** + **IIc** displayed the overlap of both conformers. **IIa** (red) as well as **IIb** (orange) and **IIc** (green) represent the top and conformation derived from the docking results for each monomer (overlapped with **II**). (For interpretation of the references to colour in this figure legend, the reader is referred to the web version of the article.)

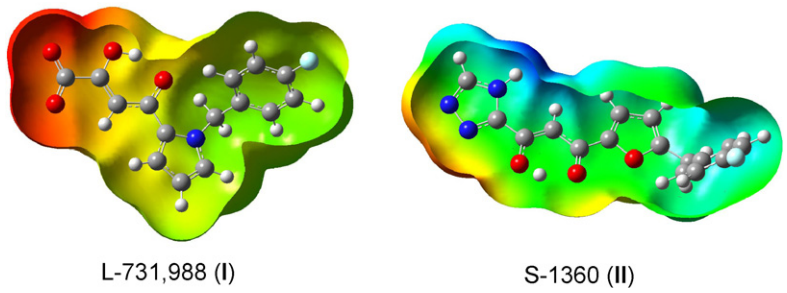

Fig. 5. MEPs derived from B3LYP/6–311G calculations for the L-731,988 and S-1360 inhibitor. The increase of negative charges comes from the blue (positive) to red (negative). (For interpretation of the references to colour in this figure legend, the reader is referred to the web version of the article.)

Table 2
Inhibition of HIV-1 integrase catalytic activities of title compounds.

Compounds	3′-Processing IC_{50} (μM)	Strand transfer IC_{50} (μM)	SI[a]
I[b]	15.2 ± 2	0.54 ± 0.08	28
Ia	12.3 ± 3.2	0.82 ± 0.06	15
Ib	28.3 ± 4.7	3.57 ± 0.51	8
Ic	25	3.7	6.7
II[c]	11 ± 2	0.6 ± 0.1	18

[a] Selectivity index. Values are from average of two or three independent experiments.
[b] From Sechi et al. (2006).
[c] From Al-Mawsawi et al. (2007).

charge distributions. In fact, the charges on some key atoms are important both in QSAR studies and in supporting mechanistic hypotheses. Fig. 5 displays the three-dimensional molecular electrostatic potential (MEP) surfaces for L-731,988 and S-1360, which were generated from the BLYP/MM optimized structures. The most nucleophilic regions (negative electronic potential) are shown in red, while the most electrophilic regions (positive electrostatic potential) are shown in blue. A more intense region of negative electrostatic potential around the 2-enol and carboxylate group of L-731,988 was observed. Otherwise, the triazole ring of S-1360 shows a bit of a positive electrostatic potential. These results are in agreement with those expected from the deprotonated and the neutral forms (for L-731,988 and S-1360, respectively). Moreover, these results can further explain the slightly different disposition of these inhibitors within the active site, particularly the interaction with the Mg^{2+} ion as observed.

4. Conclusion

In this study we designed and synthesized three kinds of photoprobes derived from the representative inhibitor L-731,988, and performed a synthetic route for the preparation of the S-1360 photolabeled analogues. Photoprobes **Ia-c** represent novel photoaffinity ligands, which may provide useful tools for studying enzyme interactions of the DKA inhibitor class of HIV-1 IN inhibitors.

Acknowledgements

We thank Dr Maria Orecchioni and Mr Paolo Fiori for assistance with NMR spectroscopy. MS is grateful to Fondazione Banco di Sardegna and to Università di Sassari for their partial financial support. The work in NN's laboratory was supported by funds from the Campbell Foundation.

References

Al-Mawsawi, L.Q., Fikkert, V., Dayam, R., Witvrouw, M., Burke Jr., T.R., Borchers, C.H., Neamati, N., 2006. Discovery of a small-molecule HIV-1 integrase inhibitor-binding site. Proc. Natl. Acad. Sci. U.S.A. 103, 10080–10085.

Al-Mawsawi, L.Q., Sechi, M., Neamati, N., 2007. Single amino acid substitution in HIV-1 integrase catalytic core causes a dramatic shift in inhibitor selectivity. FEBS Lett. 581, 1151–1156.

Anthony, N.J., 2004. HIV-1 integrase: a target for new AIDS chemotherapeutics. Curr. Top. Med. Chem. 4, 979–990.

Araki, M., Sakata, S., Takei, H., Makuiyama, T., 1974. A convenient method for the preparation of ketones by the reaction of Grignard reagents with carboxylic acid derivatives. Bull. Chem. Soc. Jpn. 47, 1777–1780.

Barbaro, G., Scozzafava, A., Mastrolorenzo, A., Supuran, C.T., 2005. Highly active antiretroviral therapy: current state of the art, new agents and their pharmacological interactions useful for improving therapeutic outcome. Curr. Pharm. Des. 11, 1843–1850.

Barreca, M.L., Lee, K.W., Chimirri, A., Briggs, J.M., 2003. Molecular dynamics studies of the wild-type and double mutant HIV-1 integrase complexed with the 5CITEP inhibitor: mechanism for inhibition and drug resistance. Biophys. J. 84, 1450–1463.

Billich, A., 2003. S-1360. Shionogi-GlaxoSmithKline. Curr. Opin. Invest. Drugs 4, 206–209.

Chang, G., Guida, W.C., Still, W.C., 1989. An internal coordinate Monte Carlo method for searching conformational space. J. Am. Chem. Soc. 111, 4379–4386.

Chehade, K.A.H., Spielmann, H.P., 2000. Facile and efficient synthesis of 4-azidotetrafluoroaniline: a new photoaffinty reagent. J. Org. Chem. 65, 4949–4953.

Chen, I.J., Neamati, N., MacKerell Jr., A.D., 2002. Structure-based inhibitor design targeting HIV-1 integrase. Curr. Drug Targets Infect. Disord. 2, 217–234.

Cohen, J., 2002. Therapies. Confronting the limits of success. Science 296, 2320–2324.

Cotelle, P., 2006. Patented HIV-1 integrase inhibitors (1998–2005). Recent Patents Anti-Infect. Drug Discov. 1, 1–15.

Dayam, R., Neamati, N., 2004. Active site binding modes of the β-diketoacids: a multi-active site approach in HIV-1 integrase inhibitor design. Bioorg. Med. Chem. 12, 6371–6381.

De Clercq, E., 2002. Strategies in the design of antiviral drugs. Nat. Rev. Drug Discov. 1, 13–25.

De Clercq, E., 2005. New approaches toward anti-HIV chemotherapy. J. Med. Chem. 48, 1297–1313.

Dormán, G., Prestwich, G.D., 1994. Benzophenone photophores in biochemistry. Biochemistry 33, 5661–5673.

Dormán, G., Prestwich, G.D., 2000. Using photolabile ligands in drug discovery and development. Trends Biotechnol. 18, 64–77.

Espeseth, A.S., Felock, P., Wolfe, A., Witmer, M., Grobler, J., Anthony, N., Egbertson, M., Melamed, J.Y., Young, S., Hamill, T., Cole, J.L., Hazuda, D.J., 2000. HIV-1 integrase inhibitors that compete with the target DNA substrate define a unique strand transfer conformation for integrase. Proc. Natl. Acad. Sci. U.S.A. 97, 11244–11249.

Fedan, J.S., Hogaboom, G.K., O'Donnell, J.P., 1984. Photoaffinity labels as pharmacological tools. Biochem. Pharmacol. 33, 1167–1180.

Fleming, S.A., 1995. Chemical reagents in photoaffinity labeling. Tetrahedron 51, 12479–12520.

Gasteiger, J., Marsili, M., 1980. Iterative partial equalization of orbital electronegativity—a rapid access to atomic charges. Tetrahedron 36, 3219–3228.

Gobbi, S., Cavalli, A., Negri, M., Schewe, K.E., Belluti, F., Piazzi, L., Hartmann, R.W., Recanatini, M., Bisi, A., 2007. Imidazolylmethylbenzophenons as highly potent aromatese inhibitors. J. Med. Chem. 50, 3420–3422.

Goldgur, Y., Craigie, R., Cohen, G.H., Fujiwara, T., Yoshinaga, T., Fujishita, T., Sugimoto, H., Endo, T., Murai, H., Davies, D.R., 1999. Structure of the HIV-1 integrase catalytic domain complexed with an inhibitor: a platform for antiviral drug design. Proc. Natl. Acad. Sci. U.S.A. 96, 13040–13043.

Griffin, R.J., 1996. The 4-azidobenzyloxy carbonyl function; application as a novel protecting group and potential prodrug modification for amines. J. Chem. Soc., Perkin Trans. 1, 1205–1211.

Grobler, J.A., Stillmock, K., Hu, B., Witmer, M., Felock, P., Espeseth, A.S., Wolfe, A., Egbertson, M., Bourgeois, M., Melamed, J., Wai, J.S., Young, S., Vacca, J., Hazuda, D.J., 2002. Diketo acid inhibitor mechanism and HIV-1 integrase: implications for metal binding in the active site of phosphotransferase enzymes. Proc. Natl. Acad. Sci. U.S.A. 99, 6661–6666.

Hazuda, D.J., Felock, P., Witmer, M., Wolfe, A., Stillmock, K., Grobler, J.A., Espeseth, A., Gabryelski, L., Schleif, W., Blau, C., Miller, M.D., 2000. Inhibitors of strand transfer that prevent integration and inhibit HIV-1 replication in cells. Science 287, 646–650.

Hatanaka, Y., Sadakane, Y., 2002. Photoaffinity labeling in drug discovery and developments: chemical gateway for entering proteomic frontier. Curr. Top. Med. Chem. 2, 271–288.

Keana, J.F.W., Xiong Cai, S., 1990. New reagents for photoaffinity labeling: synthesis and photolysis of functionalized perfluorophenyl azides. J. Org. Chem. 55, 3640–3647.

Knight, D.W., 1979. Formation and reactivity of bis-anions derived from furoic acids. Tetrahedron Lett. 5, 469–472.

Kotzyba-Hibert, F., Kapfer, I., Goeldner, M., 1995. Recent trends in photoaffinity labeling. Angew. Chem., Int. Ed. Engl. 34, 1296–1312.

Lei, H., Atkinson, J., 2000. Synthesis of phytyl-and-chroman-derivatized photoaffinity labels on α-tocopherol. J. Org. Chem. 65, 2560–2567.

Little, S.J., Holte, S., Routy, J.P., Daar, E.S., Markowitz, M., Collier, A.C., Koup, R.A., Mellors, J.W., Connick, E., Conway, B., Kilby, M., Wang, L., Whitcomb, J.M., Hellmann, N.S., Richman, D.D., 2002. Antiretroviral-drug resistance among patients recently infected with HIV. New Engl. J. Med. 347, 385–394.

Morris, G.M., Goodsell, D.S., Halliday, R.S., Huey, R., Hart, W.E., Belew, R.K., Olson, A.J., 1998. Automated docking using a Lamarckian genetic algorithm an empirical binding free energy function. J. Comp. Chem. 19, 1639–1662.

Morris, G.M., Goodsell, D.S., Huey, R., Olson, A., 1996. Distributed automated docking of flexible ligands to proteins: parallel application of AutoDock 2.4. J. Comput. Aided Mol. Des. 10, 293–304.

Neamati, N., Marchand, C., Pommier, Y., 2000. HIV-1 integrase inhibitors: past, present, and future. Adv. Pharmacol. 49, 147–165.

Neamati, N., 2001. Structure-based HIV-1 integrase inhibitor design: a future perspective. Expert Opin. Investig. Drugs 10, 281–296.

Neamati, N., 2002. Patented small molecule inhibitors of HIV-1 integrase: a ten-year saga. Expert Opin. Ther. Pat. 12, 709–724.

Norcross, R.D., Von Matt, P., Kolb, H.C., Bellűs, D., 1997. Synthesis of novel cyclobuthylphosphonic acids as inhibitors of imidazole glycerol phosphate dehydratase. Tetrahedron 53, 10289–10312.

Pais, G.C.G., Burke, T.R., 2002. Novel aryl diketo-containing inhibitors of HIV-1 integrase. Drugs Future 27, 1101–1111.

Pommier, Y., Johnson, A.A., Marchand, C., 2005. Integrase inhibitors to treat HIV/AIDS. Nat. Rev. Drug Discov. 4, 236–248.

Rowley, M., 2008. The discovery of raltegravir, an integrase inhibitor for the treatment of HIV infection. Prog. Med. Chem. 46, 1–28.

Sechi, M., Derudas, M., Dallocchio, R., Dessì, A., Bacchi, A., Sannia, L., Carta, F., Palomba, M., Ragab, O., Chan, C., Shoemaker, R., Sei, S., Dayam, R., Neamati, N., 2004a. Design and synthesis of novel indole β-diketo acid derivatives as HIV-integrase inhibitors. J. Med. Chem. 47, 5298–5310.

Sechi, M., Angotzi, G., Dallocchio, R., Dessì, A., Carta, F., Sannia, L., Mariani, A., Fiori, S., Sanchez, T., Movsessian, L., Plasencia, C., Neamati, N., 2004b. Design and synthesis of novel dihydroxyindole-2-carboxylic acids as HIV-1 integrase inhibitors. Antiviral Chem. Chemother. 15, 67–81.

Sechi, M., Bacchi, A., Carcelli, M., Compari, C., Duce, E., Fisicaro, E., Rogolino, D., Gates, P., Derudas, M., Al-Mawsawi, L.Q., Neamati, N., 2006. From ligand to complexes: inhibition of human immunodeficiency virus type 1 integrase by β-diketo acid metal complexes. J. Med. Chem. 49, 4248–4260.

Sechi, M., Carcelli, M., Rogolino, D., Neamati, N., 2009. Role of metals in HIV-1 integrase inhibitor design. In: HIV-1 Integrase: Mechanism of Action and Inhibitor Design, John Wiley & Sons.

Semenova, E.A., Marchand, C., Pommier, Y., 2008. HIV-1 integrase inhibitors: update and perspectives. Adv. Pharmacol. 56, 199–228.

Smith, M.E., 1921. Friedel and Crafts' reaction. The carbomethoxy-benzoyl chloride with aromatic hydrocarbon and aluminium chloride. J. Am. Chem. Soc. 43, 1920–1924.

Sotriffer, C.A., Ni, H., McCammon, A.J., 2000a. HIV-1 integrase inhibitor interactions at the active site: prediction of binding modes unaffected by crystal packing. J. Am. Chem. Soc. 122, 6136–6137.

Sotriffer, C.A., Ni, H., McCammon, A.J., 2000b. Active site binding modes of HIV-1 integrase inhibitors. J. Med. Chem. 43, 4109–4117.

Stoner, E.J., Cothron, D.A., Balmer, M.K., Roden, B.A., 1995. Benzylation via tandem Grignard reaction. Iodotrimethylsilane (TMSI) mediated reduction. Tetrahedron 51, 11043–11062.

Tanaka, A., Teresawa, T., Hagihara, H., Sakuma, Y., Ishibe, N., Sawada, M., Takasugi, H., Tanaka, H., 1998. Inhibitors of acyl-CoA: cholesterol O-acyltransferase (ACAT). Part 1: Identification and structure-activity relationship of a novel series of substituted N-alkyl-N-biphenylylmethyl-N′-arylureas. Bioorg. Med. Chem. 6, 15–30.

Vanek, T., Velkovà, V., Gut, J., 1984. Preparation of 3- and 3,5-substituted-1,2,4 triazole. Collect. Czech. Chem. Commun. 49, 2492–2495.

Wang, Y., Serradell, N., Bolos, J., Rosa, E., 2007. MK-0518, HIV integrase inhibitor. Drugs Future 32, 118–122.

Woodruf, M., Polya, J.B., 1975. Pyrazolidine-3,5-diones with heterocyclic substituents. IV. Ionization constants. Aust. J. Chem. 28, 1583–11583.

Yoshinaga, T., Sato, A., Fujishita, T., Fujiwara, T., 2002. In vitro activity of a new HIV-1 integrase inhibitor in clinical development. In: Proceedings of the 9th Conference on Retroviruses and Opportunistic Infections, Seattle, USA.

Zeinalipour-Loizidou, E., Nicolaou, C., Nicolaides, A., Kostrikis, L.G., 2007. HIV-1 integrase: from biology to chemotherapeutics. Curr. HIV Res. 5, 365–388.

Zhao, H., Neamati, N., Pommier, Y., Burke, T.R., 1997. Design and synthesis of photoactivatable coumarin-containing HIV-1 integrase inhibitors. Heterocycles 45, 2277–2282.